J10C.3

Applications of the Water Vapor Channels on GeoXO GXI

Andrew K. Heidinger *
NOAA/NESDIS GEO Senior Scientist

1. INTRODUCTION

GeoXO is the 6th version of the GOES program and will represent a major advance in capabilities from the current version, GOES-R (Lindsey et al., 2024). The imager on GeoXO, GXI, is an incremental improvement over the highly capable imager on GOES-R, ABI. While being an incremental improvement, GXI offers some significant advances over ABI. Two of these improvements are the inclusion of two new water vapor sensing bands. The first water vapor band is at 5.15 µm. It peaks lower in the atmosphere than any of existing ABI IR water vapor channels which are included on GXI. The second water vapor channel is the 0.91µm channel which is spectrally located in the 0.94µm water vapor rotation band.

Figure 1 shows a comparison of the 0.91µm band from MTG/FCI which is assumed to be the GXI band for this study. Also shown in this figure are the bands offered by MODIS in this region and spectral transmission of water vapor for the USA standard profile.

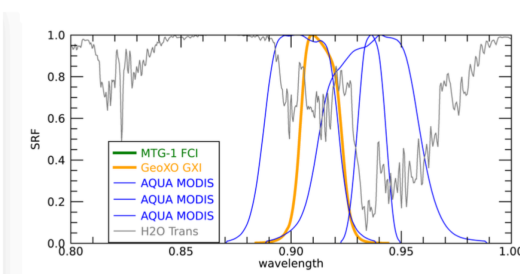

Figure 1. Comparison of the assumed GeoXO GXI 0.91µm spectral response functions to those from MTG/FCI and AQUA/MODIS. GXI is assumed to be FCI for this channel in this study.

Figure 2 shows the weighting functions for the GXI IR h_2o bands computed for the USA standard atmosphere. The dashed line shows the level where ½ of the total precipitable water (TPW) resides below. This fact illustrates the challenge of IR retrievals for low-level water vapor. Even though 5.15µm peaks much lower than the existing channels, its weighting function can be higher than 50% of the water vapor of the atmosphere. This weakness can be offset by the use of the 0.91µm channel because it is directly sensitive to the TPW and therefore provides information on the lowest levels of the atmosphere where most water resides and is most challenging to IR retrievals. In addition, the IR channels can often sense radiation from the surface and uncertainty in the surface temperature and emissivity can adversely impact IR results. The 0.91µm does not suffer from these issues. The study of the impacts of the addition of the two new channels on the retrieval of a simplified TPW profile is the goal of this paper.

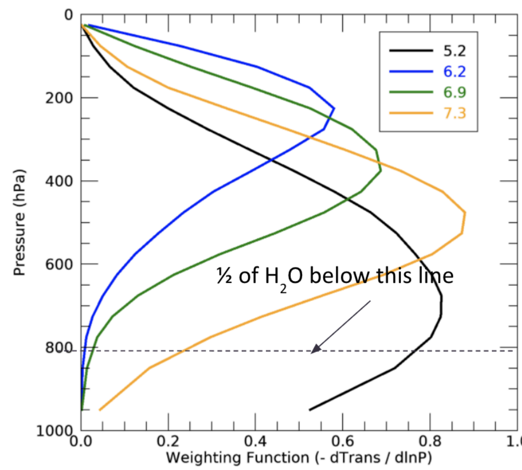

Figure 2. Weighting functions of the GeoXO GXI IR h_2o channels for the USA standard atmosphere.

2. Retrieval Model

This section will provide the methods used for radiative transfer modeling, retrievals and for assessing the impact of the new GeoXO GXI channels.

2.1 *Assumed Atmospheric Model*

Many imager based TPW retrievals will retrieve two or three layers of information on TPW and a similar number of layers for temperature. In this retrieval, we adopt a similarly simple but slightly different set of retrieved parameters. In this retrieval, we treat the temperature profile as having a linear lapse rate from from the surface to the tropopause and a uniform temperature above the tropopause. At the surface, there is a surface air temperature and a surface skin temperature that is free to vary from the surface air temperature. Figure 3 shows a representation of this simple model alongside a full profile from MERRA-2 (Molod et al., 2015). The precipitable water (PW) (integrated from a level to space) profile is assumed to be described by the total precipitable water (TPW) and its scale height (defined as the height where TPW decreases by 1/e). For the retrieval, the temperature lapse rate, surface air temperature and tropopause height are assumed known and the retrieved parameters are the surface skin temperature, the TPW and the TPW scale height.

* *Corresponding author address:Andrew K. Heidinger*, NOAA/NESDIS/GEO, Madison, WI 53706; e-mail: andrew.heidinger@noaa.gov.

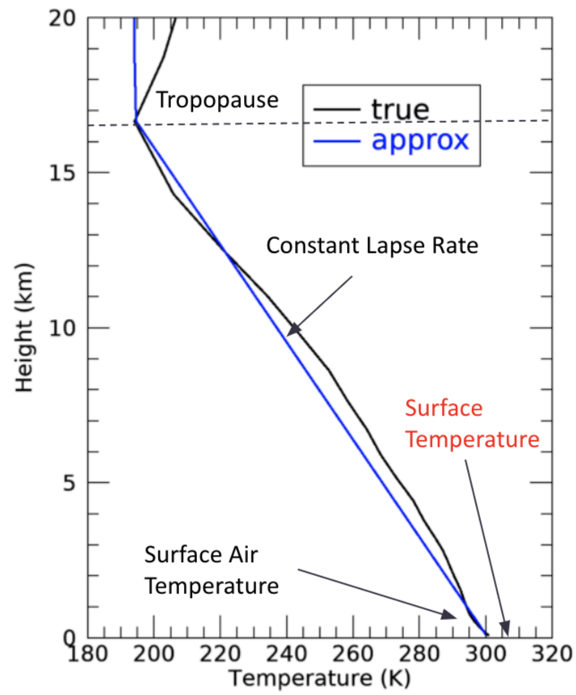

Figure 3. Example of a comparison of the assumed temperature profile and a corresponding temperature profile from the NASA MERRA-2 data.

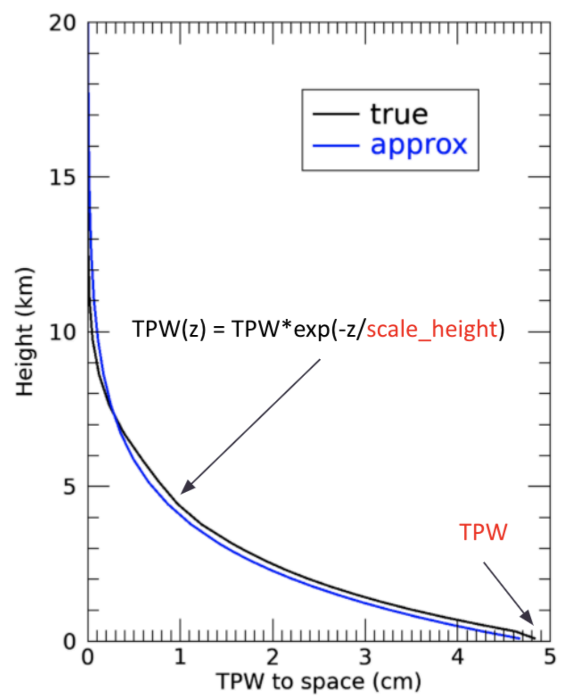

Figure 4. Same as figure 3 except for the profile of TPW integrated from each level to space.

2.1 *Radiative Transfer Model*

The radiative transfer model used here was a standard adding/doubling code using a correlated-k method for gaseous absorption. The correlated-k parameters were derived using the HITRAN 2020 spectral database for the GOES-16 ABI channels, the MTG/FCI 0.91μm and proposed 5.15μm channels. The scattering properties for water clouds come from Mie Theory while the ice cloud scattering models come from a scattering model from Ping Yang (ref). A habit of aggregated columns was used. The surface emissive and reflectance properties were taken from the MODIS white sky albedo (Moody et al., 2005) and the UW/CAMEL emissivity database (Borbas et al., 2018) convolved to these channels. The mean values from the roughly 20 land cover types (Potapov et al., 2022) were computed and used. The surface was treated as a Lambertian reflector and an isotropic emitter. While only clear-sky simulations were used here, the atmosphere allowed for two layers of cloud and an arbitrary number of levels and streams used in the simulations.

2.2 *Retrieval Details*

The above radiative transfer model and assumed atmospheric profiles were coupled together as a forward model used in the retrieval. The retrieval was conducted using a standard Optimal Estimation (OE) approach (Rodgers, 2000). In the following discussion, we employ standard OE terminology. This study will not discuss the performance of the retrieved values but will focus on the impact of the observations on the retrieval diagnostics. The forward model output, ***f***, was the brightness temperatures and reflectances for the GXI channels. The assumed atmospheric information, ***b***, was the surface air temperature, temperature lapse rate and tropopause height. The retrieved parameters, ***x***, are the surface skin temperature (Tsfc), the TPW and the TPW scale height.

The *a priori* (aka prior) ($\mathbf{x}_a$) and the prior covariance matrices ($\mathbf{S}_a$) are computed using MERRA-2 global reanalysis data. In future studies, these global values can be refined and verified using MTG/FCI data. The following text shows the prior values ($\mathbf{x}_a$)

$$\mathbf{x}_a = [\ 281.144\ (\mathrm{K}),\ 2.23\ (\mathrm{cm}^2),\ 2.5\ (\mathrm{km})\ ]$$

With the covariance terms used to construct $\mathbf{S}_a$ shown below.

Covariance Term	Value	Units
T_{sfc} vs T_{sfc}	562	K^2
TPW vs TPW	2.92	cm^2
h_{h2o} vs h_{h2o}	1.10	km^2
TPW vs T_{sfc}	28.0	cm K
T_{sfc} vs h_{h2o}	-15.1	K km
TPW vs h_{h2o}	-0.290	cm km

The 0.91µm channel was included as a ratio of the 0.91µm to the 0.86µm channel. This is commonly done to reduce the impact of surface reflectance which is similar for most surfaces for these two channels. Unless explicitly stated, the 0.91µm observation will also refer to this ratio in the retrieval. The covariance terms for the IR brightness temperatures (BTs) are computed from a global analysis of the difference between the computed and observed clear sky values. The values for the new channels are assumed. For 5.15µm, we took the value of 7.3µm and we assumed a 0.1 standard error value for the 0.91/0.86µm ratio. Once FCI data is available, this value can be refined.

Covariance Term	Value	Units
11 µm BT	$(22.0)^2$	K^2
11-12 µm BT	$(0.210)^2$	K^2
6.2 µm BT	$(3.1)^2$	K^2
6.9 µm BT	$(3.7)^2$	K^2
7.3 µm BT	$(4.6)^2$	K^2
5.15 µm BT	$(4.6)^2$	K^2
0.91/0.86 µm	$(0.1)^2$	none

The retrieval was run for assumed clear skies over the open grassland surface. The atmospheric parameters were based on the USA 1976 standard atmosphere.

2.3 *Retrieval Diagnostics*

One of the benefits of OE approaches are the diagnostics that can be computed from the standard OE matrices as outlined in Smith et al. (2021). The averaging kernel, **A**, is computed from the following equation based on the retrieved covariance matrix ($\mathbf{S_x}$), the kernel matrix (**K**) and the observation covariance matrix ($\mathbf{S_y}$).

$$\mathbf{A = S_x (K S_y^{-1} K)^T}$$

Knowing **A**, the reliance of the prior (**RoP**) matrix can be computed as follows.

$$\mathbf{RoP = 1 - S_x (K S_y^{-1} K)^T}$$

The diagonal elements of the **RoP** give values that range from 0 to 1 where 1 indicates a total reliance of the retrieved elements of **x** on its corresponding element in the prior value of $\mathbf{x_a}$ and 0 indicates no reliance.

The Shannon information content (**H**) is computed as follows.

$$\mathbf{H = -½ \log2|I\text{-}A|}$$

Finally, the degree of freedom (**DoF**) is computed using the next equation.

$$\mathbf{DoF = trace(A)}$$

For our retrieval, which has 3 retrieved parameters, **DoF** will vary from 0 to 3.

3. Predicted Impact of New Channels

Using the diagnostic terms described above, we can explore the impact of the new h_2o channels on GXI to retrieve the TPW profile within the context of the assumed retrieval model. In the following analysis, the retrieval metrics of RoP, H and DoF are computed for 7 different combinations of channels. The first channel combination is a single 11µm retrieval. The second retrieval added in the 12µm. The third through fifth combinations add in the 6.2, 6.9 and 7.3 µm channels sequentially. The sixth combination added in the new 5.15µm channel and seventh and final combination added in the 0.91µm channel.

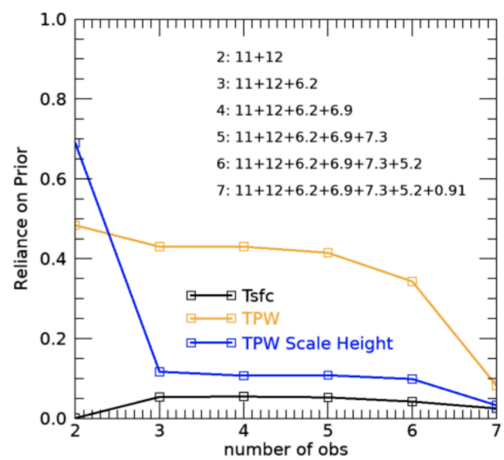

Figure 5. Reliance on Prior (RoP) for each of the three retrieved variables as a function of channels used in the retrieval.

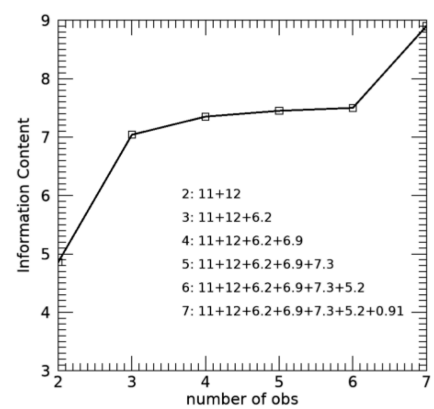

Figure 6. Information Content (H) as a function of channels used in the retrieval.

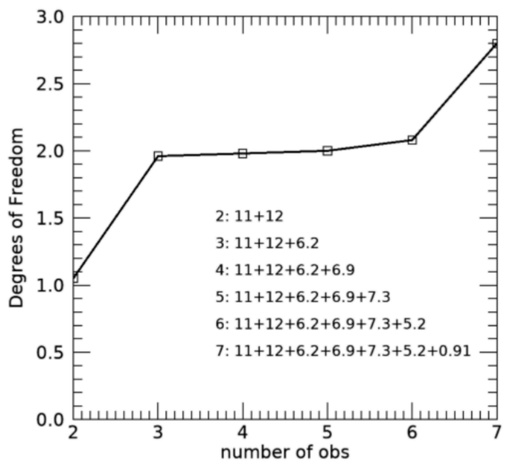

Figure 7. Degrees of Freedom (DoF) as a function of channels used in the retrieval.

The results of Figures 5, 6 and 7 are consistent and show the expected positive impact of adding channels. They show that addition of the 5.15µm is very impactful and more impactful than the incremental impacts of adding any of the other previous IR h_2o channels. However, the largest impact by far is seen with the addition of the 0.91µm channel. Addition of this channel greatly reduces the reliance on prior knowledge, increases H from 7 to almost 9 and increases the DoF from 2 to about 2.75.

4. CONCLUSIONS

These results show the additional information on lower level water vapor offered by GXI should provide significant benefit to estimating TPW profiles. Because the 0.91µm channel provides a sensitivity to the total TPW which is lacking in the IR h_2o channels and is insensitive to errors in the surface temperature and emissivity, this new channel provides the most benefit for daytime land retrievals of the simplified TPW profile. We looked forward to testing these concepts from a geostationary orbit with the MTG/FCI data.

5. REFERENCES

Borbas, E. Eva, Glynn Hulley, Michelle Feltz, Robert Knuteson, and Simon Hook. 2018. "The Combined ASTER MODIS Emissivity over Land (CAMEL) Part 1: Methodology and High Spectral Resolution Application" Remote Sensing 10, no. 4: 643. https://doi.org/10.3390/rs10040643

Lindsey, D. T., and Coauthors, 2024: GeoXO: NOAA's Future Geostationary Satellite System. Bull. Amer. Meteor. Soc., https://doi.org/10.1175/BAMS-D-23-0048.1, in press.

Molod, A., Takacs, L., Suarez, M., Bacmeister, J.. 2015. Development of the GEOS-5 atmospheric general circulation model: evolution from MERRA to MERRA2. Geoscientific Model Development. Vol. 8, No. 5, pp. 1339-1356. DOI: 10.5194/gmd-8-1339-2015

Moody, E. G., M. D. King, S. Platnick, C. B. Schaaf, and F. Gao, 2005: Spatially complete global spectral surface albedos: Value-added datasets derived from Terra MODIS land products. IEEE Transactions on Geoscience and Remote Sensing, Vol. 43, 144-158)

Potapov P., Hansen M.C., Pickens A., Hernandez-Serna A., Tyukavina A., Turubanova S., Zalles V., Li X., Khan A., Stolle F., Harris N., Song X.-P., Baggett A., Kommareddy I., Kommareddy A. (2022) The global 2000-2020 land cover and land use change dataset derived from the Landsat archive: first results. Frontiers in Remote Sensing [https://doi.org/10.3389/frsen.2022.856903]

C. D. Rodgers, Inverse Methods for Atmospheric Sounding - Theory and Practice, Singapore:World Scientific Press, 2000.

W. L. Smith et al., "Hyperspectral Satellite Radiance Atmospheric Profile Information Content and Its Dependence on Spectrometer Technology," in IEEE Journal of Selected Topics in Applied Earth Observations and Remote Sensing, vol. 14, pp. 4720-4736, 2021, doi: 10.1109/JSTARS.2021.3073482.